PHYSICAL REVIEW B **76**, 193401 (2007)

Impurity scattering and Mott's formula in graphene

Tomas Löfwander and Mikael Fogelström
Department of Microtechnology and Nanoscience, Chalmers University of Technology, S-412 96 Göteborg, Sweden

(Received 10 September 2007; published 7 November 2007)

We present calculations of the thermal and electric linear response in graphene, including disorder in the self-consistent t-matrix approximation. For strong impurity scattering, near the unitary limit, the formation of a band of impurity states near the Fermi level leads to that Mott's relation holds at low temperature. For higher temperatures, there are strong deviations due to the linear density of states. The low-temperature thermopower is proportional to the inverse of the impurity potential and the inverse of the impurity density. Information about impurity scattering in graphene can be extracted from the thermopower, either measured directly or extracted via Mott's relation from the electron-density dependence of the electric conductivity.

DOI: 10.1103/PhysRevB.76.193401 PACS number(s): 72.10.−d, 72.20.Dp, 81.05.Uw

The recent isolation of the two-dimensional one-atom thick honeycomb crystal of carbon,[1] called graphene, has generated tremendous interest partly because of the potential of carbon-based nanoscale electronics, but also for fundamental reasons.[2–16] Recent experiments[2–4] have shown that the charge conductance of graphene reaches a universal value $4e^2/h$ at low temperatures. It has also been found that the conductivity is linearly dependent on the electron density. Furthermore, an unconventional half-integer quantum Hall effect has been discovered.

All these results are nicely in line with theoretical results based on an effective low-energy theory of graphene within which charge carriers are massless Dirac fermions.[16–27] The low-temperature conductivity of graphene is most probably limited by scattering against impurities, such as vacancies or other imperfections.[4,21–25] For strong scattering, in the unitary limit, a band of impurity states centered at the Dirac point is formed.[22,23,28–31] For small temperatures, compared with the impurity bandwidth, the conductivity is predicted[19–23] to reach a minimal universal value $4e^2/(\pi h)$. Within the same model of strong impurity scattering, the conductivity varies linearly with charge density for chemical potential shifts that are large compared with the impurity bandwidth.[23] In contrast, linear dependence is absent for weak impurity scattering.[23] In a slightly different scenario, randomly distributed Coulomb scatterers are predicted to lead to similar properties.[25]

The origin of the scattering that limits the conductivity in graphene is at present controversial. Measurements of other quantities than the conductivity is most probably needed, since the conductivity, being universal, loses information about impurities at low temperatures. In this Brief Report, we show that the thermopower can provide valuable information about impurities in graphene. We also discuss the applicability of Mott's relation to graphene. After initial confirmation of this relation (and its approximate high-temperature form derived below) through experiments on thermoelectricity, it can be used to analyze the charge conductivity.

The related Nernst signal that appears in a magnetic field was studied theoretically in Ref. 21. Further properties of the thermopower in a magnetic field was studied in Ref. 32 in the strict unitary limit for which the thermopower vanishes at charge neutrality. If vacancies are strong scattering centers, the impurity potential is large, estimated, e.g., by graphene's vacuum level. Near unitary scattering can occur, although the strict unitary limit cannot, in reality, be reached. This has a big impact on the thermopower, as the impurity band is shifted from the Dirac point which leads to a large electron-hole asymmetry.[28–31] Here, we explore the consequences of such asymmetry in detail with the goal of extracting information about impurities in graphene from transport.

The starting point for the calculations is the tight-binding model for clean graphene,[17,18]

$$H_0 = -t\sum_{\langle ij\rangle}(a_i^\dagger b_j + b_j^\dagger a_i), \tag{1}$$

where t is the nearest neighbor hopping amplitude. The operators $a_i^\dagger$ and $b_j^\dagger$ create electrons on sites i and j in the graphene honeycomb lattice. The fact that this lattice can be considered as two displaced triangular lattices, with a unit cell consisting of two atoms, here denoted A and B, is made explicit by the introduction of the two creation operators. In reciprocal space, the Fermi surface is reduced to two inequivalent so-called K points at the corners of the first Brillouin zone, which we find at $\mathbf{K}_\nu = 4\pi\nu\hat{k}_x/(3\sqrt{3}a)$, where a is the nearest neighbor distance, $\nu=\pm1$, and $\hat{k}_x$ is unit vector along the k_x axis. At low energies $\epsilon \ll t$, the dispersion is linear around these points, $\epsilon(\boldsymbol{\kappa}) \approx \pm v_f|\boldsymbol{\kappa}|$, where $\boldsymbol{\kappa}$ is the k vector measured relative to the K point and $v_f = 3at/2$ is the Fermi velocity. The clean limit retarded Green's function in the K-point (low-energy) approximation is the inverse of the 2×2 (in the space of the atoms A and B) Dirac Hamiltonian matrix and has the form[22]

$$\hat{G}_\nu^{R(0)}(\boldsymbol{\kappa},\epsilon) = \frac{1}{2}\sum_{\lambda=\pm1}\frac{1}{\epsilon - \lambda v_f|\boldsymbol{\kappa}| + i0^+}\begin{pmatrix} 1 & \lambda\nu e^{-i\nu\beta} \\ \lambda\nu e^{i\nu\beta} & 1 \end{pmatrix},$$

where $\beta = \arg(\kappa_x + i\kappa_y)$ is an angle defining the direction of the vector $\boldsymbol{\kappa}$ with respect to the k_x axis.

We include impurities by adding

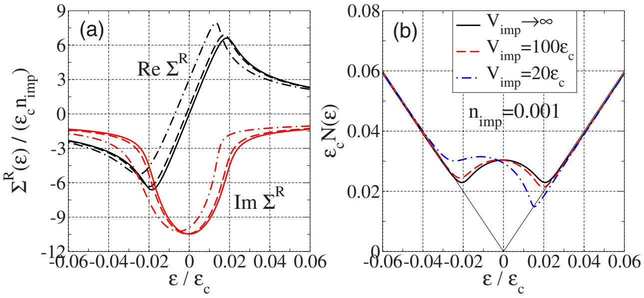

FIG. 1. (Color online) (a) The impurity self-energy and (b) the density of states for large impurity potential V_{imp}. An impurity band of width $\gamma \sim \epsilon_c \sqrt{n_{\text{imp}}}$ is formed near the Fermi level at an energy $\epsilon_r \sim \epsilon_c^2 / V_{\text{imp}}$. For $\epsilon \gg \gamma$, the spectrum is linear.

$$H_{\text{imp}} = \sum_{i=1}^{N_{\text{imp}}^{A}} V_{\text{imp}} a_i^{\dagger} a_i + \sum_{j=1}^{N_{\text{imp}}^{B}} V_{\text{imp}} b_j^{\dagger} b_j \tag{2}$$

to the Hamiltonian, where V_{imp} is the impurity strength. The numbers of impurities N_{imp} in the two sublattices A and B are assumed approximately equal and small compared with the number N of unit cells in the crystal. In the dilute limit, when we only keep terms of first order in the density $n_{\text{imp}} = N_{\text{imp}}/N$, crossing diagrams are neglected when the configuration average is performed over the random distribution of impurities.[33] The resulting self-energy is written in terms of a t matrix $\hat{\Sigma}^R(\epsilon) = n_{\text{imp}} \hat{T}^R(\epsilon)$, where

$$\hat{T}^R(\epsilon) = V_{\text{imp}} \left[\hat{1} - \left(\frac{V_{\text{imp}}}{N} \right) \sum_{\mathbf{k}} \hat{G}^R(\mathbf{k}, \epsilon) \right]^{-1}. \tag{3}$$

The sum over $\mathbf{k}$ can be performed analytically in the K-point approximation. The off-diagonal components vanish, the resulting self-energy is diagonal, and the average Green's function is $(1/N)\Sigma_{\mathbf{k}} \hat{G}^R(\mathbf{k}, \epsilon) = \hat{1}(z/\epsilon_c^2)\log[-z^2/(\epsilon_c^2 - z^2)]$, where $z = \epsilon - \Sigma^R(\epsilon)$. The energy cutoff ϵ_c is related to the cutoff k_c in reciprocal space below which the dispersion is linear.

We plot the self-consistent self-energy and the resulting density of states in Fig. 1. In the unitary limit, defined as $V_{\text{imp}} \to \infty$, a band of impurity states is formed centered at the Dirac point.[22,23,28–31] The bandwidth, estimated by $\gamma = -\Im \Sigma^R(0)$, is computed by solving the equation $(2\gamma^2/\epsilon_c^2)\ln(\epsilon_c/\gamma) = n_{\text{imp}}$. To logarithmic accuracy, γ scales as $\sqrt{n_{\text{imp}}}$. For V_{imp} deviating from the unitary limit, the impurity band is shifted away from the Fermi level to an energy ϵ_r. The self-energy is approximated as $\Sigma^R(\epsilon) = -i\gamma + \alpha(\epsilon - \epsilon_r) + \cdots$ for small energies, $\epsilon - \epsilon_r \ll \gamma$. To lowest order, we have $\epsilon_r = -\epsilon_c^2/(2V_{\text{imp}}[\ln(\epsilon_c/\gamma) - 1])$ and $\alpha = \alpha_0/(1+\alpha_0)$, where $\alpha_0 = (1/n_{\text{imp}})(2\gamma^2/\epsilon_c^2)[\ln(\epsilon_c/\gamma) - 1]$ is only weakly (logarithmically) dependent on the density of impurities. The shift of the impurity band away from the Fermi level by the amount ϵ_r leads to a large electron-hole asymmetry and the anomalous thermoelectric response that we study below. For large energies, $\epsilon \gg \gamma$, the density of states is essentially the same as in the clean limit.

Next nearest neighbor hopping (t') gives an electron-hole asymmetric contribution to the dispersion, but it enters in second order in the low-energy expansion: $\epsilon(\boldsymbol{\kappa}) = \pm v_f |\boldsymbol{\kappa}| + v_f^2 |\boldsymbol{\kappa}|^2 [t'/t^2 \mp \nu \cos(3\beta)/(6t)] + \cdots$. These contributions are only important far from the Fermi level and we neglect them.

The linear response is defined as[33]

$$\begin{pmatrix} \mathbf{j} \\ \mathbf{j}_E \end{pmatrix} = \begin{pmatrix} \mathcal{L}_{11} & \mathcal{L}_{12} \\ \mathcal{L}_{21} & \mathcal{L}_{22} \end{pmatrix} \left(\begin{array}{c} \dfrac{\mathbf{E}}{T} \\[2ex] \nabla \dfrac{1}{T} \end{array} \right), \tag{4}$$

where $\mathbf{E}$ is the electric field and T is the temperature. The Onsager relation $\mathcal{L}_{12} = \mathcal{L}_{21}$ holds. The charge conductivity is defined as $\sigma = e^2 \mathcal{L}_{11}/T$, while the electronic contribution to the open-circuit heat conductivity is $\kappa^{el} = (1/T)(\mathcal{L}_{22} - \mathcal{L}_{12}^2/\mathcal{L}_{11})$. Finally, the thermopower is defined as $S = -\mathcal{L}_{12}/(eT\mathcal{L}_{11})$. The response functions $\mathcal{L}_{ij}$ are defined in terms of Kubo formulas, i.e., current-current correlation functions. The charge current operator for graphene modeled as above has the simple form $\mathbf{j} = \Sigma_{\mathbf{k}}[\mathbf{v}_{\mathbf{k}} a_{\mathbf{k}}^{\dagger} b_{\mathbf{k}} + \text{H.c.}]$, where H.c. denotes Hermitian conjugate, and $\mathbf{v}_{\mathbf{k}} = \nabla_{\mathbf{k}} \phi_{\mathbf{k}}$. Note that the function $\phi_{\mathbf{k}} = -t \Sigma_{j=1}^{3} e^{i\mathbf{k}\cdot\boldsymbol{\delta}_j}$ and, therefore, also $\mathbf{v}_{\mathbf{k}}$ are complex functions since the three nearest neighbor vectors $\boldsymbol{\delta}_j$ point in three directions rotated 120° relative to each other in the graphene plane. The heat current operator has an extra term from impurity scattering, $\mathbf{j}_E = \mathbf{j}_E^0 + \mathbf{j}_E^{\text{imp}}$, where $\mathbf{j}_E^0 = (1/2)\Sigma_{\mathbf{k}}(\mathbf{v}_{\mathbf{k}}\phi_{\mathbf{k}}^* + \mathbf{v}_{\mathbf{k}}^*\phi_{\mathbf{k}})(a_{\mathbf{k}}^{\dagger} a_{\mathbf{k}} + b_{\mathbf{k}}^{\dagger} b_{\mathbf{k}})$ and $\mathbf{j}_E^{\text{imp}} = (1/2)\Sigma_{\mathbf{kq}}[(U_{\mathbf{q}}^{B}\mathbf{v}_{\mathbf{k}} + U_{\mathbf{q}}^{A}\mathbf{v}_{\mathbf{k+q}}) a_{\mathbf{k}}^{\dagger} b_{\mathbf{k+q}} + \text{H.c.}]$, where $U_{\mathbf{q}}^{A} = (V_{\text{imp}}/N)\Sigma_i e^{-i\mathbf{q}\cdot\mathbf{A}_i}$ is the Fourier transform of the impurity potential, including phase shifts in the sum over impurity sites $\mathbf{A}_i$ (and equivalently for the B sublattice). This, in principle, complicates the calculation of the thermal response. However, for graphene, as was shown for normal metals by Jonson and Mahan[34,35] (see also Ref. 36), the response function kernels are simply related to each other: Once we know the charge current response kernel $K_{11} = K(\epsilon)$, we get the other two kernels through $K_{12} = \epsilon K(\epsilon)$ and $K_{22} = \epsilon^2 K(\epsilon)$. The response functions are then computed by integration

$$\mathcal{L}_{ij} = \frac{1}{\pi^2} \int_{-\infty}^{\infty} d\epsilon \left(-\frac{\partial f(\epsilon)}{\partial \epsilon} \right) K_{ij}(\epsilon), \tag{5}$$

where $f(\epsilon)$ is the Fermi distribution function. For point scatterers, the kernel $K(\epsilon)$ can be approximated by the bare bubble.[22,23] The needed sum over $\mathbf{k}$ can be computed analytically in the K-point approximation. We write $z = \epsilon - \Sigma^R(\epsilon) = a(\epsilon) + ib(\epsilon)$ and find[22,33]

$$\begin{aligned} K(\epsilon) = 1 + \frac{a^2 + b^2}{ab} \arctan \frac{a}{b} - \sum_{s=\pm 1} s \Bigg[& \frac{a(\epsilon_c + sa) + sb^2}{(\epsilon_c + sa)^2 + b^2} \\ & - \frac{a^2 + b^2}{2ab} \arctan \left(\frac{\epsilon_c + sa}{b} \right) \Bigg]. \end{aligned} \tag{6}$$

In Fig. 2, we present results for conductivities and the thermopower. The conductivities are only weakly dependent on the exact value of V_{imp} as long as $V_{\text{imp}} \gg \epsilon_c$, as is clear when we compare the solid and dotted lines in Figs. 2(a) and 2(b). These response functions are given by the electron-hole symmetric part of $K(\epsilon)$, which is robust as long as the impu-

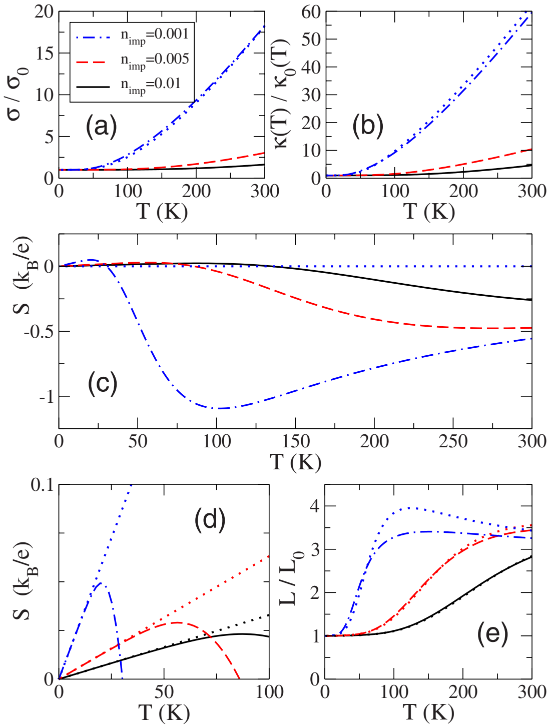

FIG. 2. (Color online) Temperature dependence of (a) the charge conductance, (b) the heat conductance, and (c) the thermopower for three values of the impurity density $n_{\rm imp}$. The solid and broken lines are for a large impurity potential $V_{\rm imp}=20\epsilon_c$, while the dotted lines are for the strict unitary limit $V_{\rm imp}\to\infty$. In (a) and (b), we have normalized the conductivities by the low-temperature asymptotics $\sigma_0=4e^2/(\pi h)$ and $\kappa_0(T)=4\pi k_B^2T/(3h)$. In (d), we show the details at low temperatures. The dotted lines are the thermopower computed through the Mott relation. In (e), we show the Lorenz ratio $L=\kappa/(\sigma T)$ in units of the value $L_0=(\pi^2/3)(k_B^2/e^2)$ appearing in Wiedemann-Franz law. We used $\epsilon_c=1$ eV → 11 605 K to convert the temperature scale to Kelvin.

rity band is not shifted far from the Dirac point. We conclude that, for these response functions, the unitary limit is effectively approached quickly for $V_{\rm imp}\gg\epsilon_c$. On the other hand, the thermopower is given by the electron-hole asymmetric part of $K(\epsilon)$ and is very sensitive to impurity scattering. We have $S(-V_{\rm imp})=-S(V_{\rm imp})$. The order of magnitude $S\sim k_B/e \sim 100\ \mu\text{V/K}$ is in agreement with experiments on single-walled carbon nanotubes.[37]

At low temperatures, both the charge conductivity and the slope of the thermal conductivity reach constant universal values $\sigma_0=4e^2/(\pi h)$ and $\kappa_0=4\pi k_B^2T/(3h)$, respectively, that are independent of the details of the impurities, in agreement with results in the literature.[19–23] On the other hand, the low-temperature slope of the thermopower reaches a nonuniversal constant value that depends sensitively on the nature of impurity scattering. These results are understood in terms of a Sommerfeld expansions of the transport coefficients in the small parameter $T/\gamma\ll 1$ for slowly varying kernels $K_{ij}(\epsilon)=K_{ij}(0)+\epsilon K'_{ij}(\epsilon)|_{\epsilon=0}+\cdots$. The needed parts of the kernel [Eq. (6)] can be computed analytically, $K(0)=2$ and $K'(0)=4\alpha(1-\alpha)\epsilon_r/(3\gamma^2)$, where we assumed that $\epsilon_r\ll\gamma\ll\epsilon_c$. The universal conductivities immediately follow, and the low-temperature thermopower is (reinstating $\hbar$ and k_B)

$$S \simeq -\frac{\pi^2}{3}\frac{2\alpha(1-\alpha)\epsilon_r}{3\gamma^2}\frac{k_B^2T}{e}. \qquad (7)$$

This means that at low temperatures, $k_BT\ll\gamma$, the Wiedemann-Franz law is obeyed, $L=\kappa^{el}/\sigma T=L_0=(\pi^2/3)(k_B^2/e^2)$, and also the Mott formula holds, $S=-(\pi^2/3)(k_B^2T/e)\,d[\ln K(\epsilon)]/d\epsilon|_{\epsilon\to 0}$. At higher temperatures, $T\gtrsim\gamma$, however, neither of these relations hold, see Figs. 2(d) and 2(e). This happens for any system where the conductivity kernel is varying around the Fermi level on some particular energy scale, here given by the impurity bandwidth γ. For normal metals, this scale is typically given by the much larger Fermi energy.

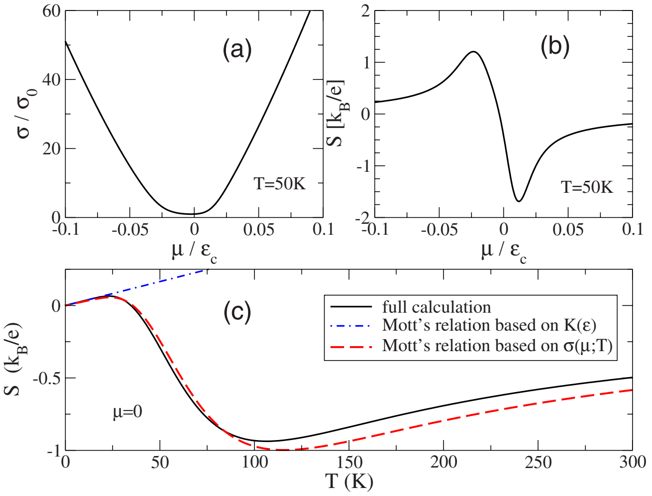

FIG. 3. (Color online) The charge conductance (a) and the thermopower (b) as function of chemical potential at $T=50$ K. In (c), we show how thermal smearing leads to an approximate Mott's relation based on the charge conductance as function of chemical potential. For $T\ll\gamma$, the Mott relation is exact to leading order (dash-dotted line).

There are other contributions to the heat conductance besides the electronic. In particular, phonons are important in graphite and carbon nanotubes,[38] for which the Lorenz ratio is typically found to be $L\sim 10L_0-100L_0$.

In contrast, the thermopower is given entirely by electronic contributions. In the low-temperature limit, $T\ll\gamma$, we see that S is proportional to ϵ_r and γ^{-2}, where for large $V_{\rm imp}\gg\epsilon_c$, $\epsilon_r\propto\epsilon_c^2/V_{\rm imp}$ and $\gamma\propto\epsilon_c\sqrt{n_{\rm imp}}$. The thermopower is therefore proportional to the inverses $1/V_{\rm imp}$ and $1/n_{\rm imp}$. In the strict unitary limit, $V_{\rm imp}\to\infty$, when electron-hole symmetry is restored, the thermopower vanishes.[21,32] However, for a large (but not infinitely large) impurity potential, the thermopower is enhanced: the smallness of $1/V_{\rm imp}$ is compensated by the large $1/n_{\rm imp}$. This also means that if $n_{\rm imp}$ can be controlled, $V_{\rm imp}$ can be extracted by measuring the slope of the thermopower at low temperatures.

We note that there are clear analogies with the situation in a d-wave superconductor,[39] where the Lorenz ratio deviates from L_0 but recovers at low temperatures, $T\ll\gamma$. An anomalously large thermoelectric coefficient $\mathcal{L}_{12}$ has been predicted.[40,41] A significant difference for graphene compared with the superconducting case is the possibility to measure the thermoelectric response directly through the thermopower, which is not possible in a superconductor since supercurrents short circuit the thermoelectric voltage.

The chemical potential of graphene can be tuned by applying a voltage to the substrate.[1] We show the dependence on the chemical potential in Figs. 3(a) and 3(b). The charge conductance as function of μ is essentially linear at large μ. The value of the thermopower at $\mu=0$ and the associated asymmetry of S around $\mu=0$, and also around the point μ^*, where $S(\mu^*)=0$, are related to the amount of electron-hole asymmetry caused by impurity scattering.

Mott's formula, derived mathematically through the Sommerfeld expansion, is only valid at low temperatures, $T \ll \gamma$, since the conductivity kernel $K(\epsilon)$ varies slowly only on the energy scale γ. However, as we show in Fig. 3(c), it turns out that thermal smearing leads to an effective, approximate Mott relation $S \approx -(\pi^2/3)(k_B^2 T/e) d[\ln \sigma(\mu;T)]/d\mu$ in terms of the full temperature dependent conductivity. The nonlinear temperature dependence $S(T)$ is obtained at $\mu=0$.

In summary, we have presented results for the linear response to electric and thermal forces in graphene for the case of strong impurity scattering near the unitary limit. The impurity band of width γ is centered near the Fermi level, at an energy $\epsilon_r \propto \epsilon_c^2 / V_{\text{imp}}$. The induced electron-hole asymmetry gives small changes of the charge and thermal conductivities but leads to an enhanced thermopower, which at low temperatures, $T \ll \gamma$, is linear in temperature with a slope proportional to $1/(V_{\text{imp}} n_{\text{imp}})$. The thermopower, measured directly or estimated by Mott's relation can therefore be used to extract information about impurity scattering in graphene.

It is a pleasure to thank A. Yurgens and V. Shumeiko for valuable discussions. Financial support from SSF, the Swedish Foundation for Strategic Research (T.L.), and the Swedish Research Council (M.F.) is gratefully acknowledged.

---

[1] K. S. Novoselov, A. K. Geim, S. V. Morozov, D. Jiang, Y. Zhang, S. V. Dubonos, I. V. Grigorieva, and A. A. Firsov, Science **306**, 666 (2004).

[2] K. S. Novoselov, A. K. Geim, S. V. Morozov, D. Jiang, M. I. Katsnelson, I. V. Grigorieva, S. V. Dubonos, and A. A. Firsov, Nature (London) **438**, 197 (2005).

[3] Y. Zhang, Y.-W. Tan, H. L. Stormer, and P. Kim, Nature (London) **438**, 201 (2005).

[4] A. K. Geim and K. S. Novoselov, Nat. Mater. **6**, 183 (2007).

[5] C. Berger *et al.*, Science **312**, 1191 (2006).

[6] A. C. Ferrari *et al.*, Phys. Rev. Lett. **97**, 187401 (2006).

[7] H. B. Heersche, P. Jarillo-Herrero, J. B. Oostinga, L. M. K. Vandersypen, and A. F. Morpurgo, Nature (London) **446**, 56 (2007).

[8] A. Bostwick, T. Ohta, T. Seyller, K. Horn, and E. Rotenberg, Nat. Phys. **3**, 36 (2007).

[9] F. Schedin, K. S. Novoselov, S. V. Morozov, D. Jiang, E. H. Hill, P. Blake, and A. K. Geim, Nat. Mater. **6**, 652 (2007).

[10] Z. Chen, Y.-M. Lin, M. J. Rooks, and P. Avouris, arXiv:cond-mat/0701599 (unpublished).

[11] B. Trauzettel, D. V. Bulaev, D. Loss, and G. Burkard, Nat. Phys. **3**, 192 (2007).

[12] A. Rycerz, J. Tworzydlo, and C. W. J. Beenakker, Nat. Phys. **3**, 172 (2007).

[13] V. V. Cheianov, V. Fal'ko, and B. L. Altshuler, Science **315**, 1252 (2007).

[14] Y.-W. Son, M. L. Cohen, and S. G. Louie, Nature (London) **444**, 347 (2006).

[15] P. G. Silvestrov and K. B. Efetov, Phys. Rev. Lett. **98**, 016802 (2007).

[16] M. I. Katsnelson, Mater. Today **10**, 20 (2007).

[17] P. R. Wallace, Phys. Rev. **71**, 622 (1947).

[18] J. C. Slonczewski and P. R. Weiss, Phys. Rev. **109**, 272 (1958).

[19] N. H. Shon and T. Ando, J. Phys. Soc. Jpn. **67**, 2421 (1998).

[20] V. P. Gusynin and S. G. Sharapov, Phys. Rev. Lett. **95**, 146801 (2005).

[21] V. P. Gusynin and S. G. Sharapov, Phys. Rev. B **73**, 245411 (2006).

[22] N. M. R. Peres, F. Guinea, and A. H. Castro Neto, Phys. Rev. B **73**, 125411 (2006).

[23] P. M. Ostrovsky, I. V. Gornyi, and A. D. Mirlin, Phys. Rev. B **74**, 235443 (2006).

[24] K. Ziegler, Phys. Rev. Lett. **97**, 266802 (2006).

[25] K. Nomura and A. H. MacDonald, Phys. Rev. Lett. **98**, 076602 (2007).

[26] S. Das Sarma, E. H. Hwang, and W.-K. Tse, Phys. Rev. B **75**, 121406(R) (2007).

[27] T. Ando, J. Phys. Soc. Jpn. **74**, 777 (2005).

[28] G. D. Mahan, Phys. Rev. B **69**, 125407 (2004).

[29] Y. G. Pogorelov, arXiv:cond-mat/0603327 (unpublished).

[30] T. O. Wehling, A. V. Balatsky, M. I. Katsnelson, A. I. Lichtenstein, K. Scharnberg, and R. Wiesendanger, Phys. Rev. B **75**, 125425 (2007).

[31] Yu. V. Skrypnyk and V. M. Loktev, Phys. Rev. B **73**, 241402(R) (2006).

[32] B. Dóra and P. Thalmeier, Phys. Rev. B **76**, 035402 (2007).

[33] G. D. Mahan, *Many-Particle Physics*, 2nd ed. (Plenum, New York, 1990).

[34] M. Jonson and G. D. Mahan, Phys. Rev. B **21**, 4223 (1980).

[35] M. Jonson and G. D. Mahan, Phys. Rev. B **42**, 9350 (1990).

[36] I. Paul and G. Kotliar, Phys. Rev. B **67**, 115131 (2003).

[37] J. P. Small, K. M. Perez, and P. Kim, Phys. Rev. Lett. **91**, 256801 (2003).

[38] M. S. Dresselhaus and P. C. Eklund, Adv. Phys. **49**, 705 (2000).

[39] M. J. Graf, S.-K. Yip, J. A. Sauls, and D. Rainer, Phys. Rev. B **53**, 15147 (1996).

[40] T. Löfwander and M. Fogelström, Phys. Rev. B **70**, 024515 (2004).

[41] T. Löfwander and M. Fogelström, Phys. Rev. Lett. **95**, 107006 (2005).